Contrib. Astron. Obs. Skalnaté Pleso **56/2**, 55 – 81, (2026)
https://doi.org/10.31577/caosp.2026.56.2.55

New variable stars from TESS sectors 77 & 79

A. Dzygunenko[1], N. Telekh[2], K. Liashenko[3], A. Mosiichuk[4], D. Zazubyk[5], D. Tvardovskyi[6], V. Smorodska[6], V. Udovychenko[6], V. Zadubets[6], M. Yatsiuk[7] and V. Boyko[8]

[1] *American Academy in Prague, Kloboučnická 1425/13 str., 14000, Prague, Czech Republic (E-mail: andridzigunenko@gmail.com)*

[2] *III Adam Mickiewicz Secondary School in Katowice, 11 Adama Mickiewicza str., 40-092 Katowice, Poland*

[3] *National Aerospace University "Kharkiv Aviation Institute", 17 Vadym Manko str., 61000 Kharkiv, Ukraine*

[4] *Zhytomyr Higher Professional Technological School, 72 Serhiy Parajanov str., 10001, Zhytomyr, Ukraine*

[5] *Taras Shevchenko National University of Kyiv, 60 Volodymyrska str., 01601, Kyiv, Ukraine*

[6] *Citizen scientist*

[7] *Lyceum 63, 10 Ivan Vyhovsky str., 04136, Kyiv, Ukraine*

[8] *Akhiezer Institute for Theoretical Physics, National Scientific Center, Kharkiv Institute of Physics and Technology, 1 Akademichna str., 61108, Kharkiv, Ukraine*

Received: May 12, 2025; Accepted: December 10, 2025

Abstract. In this research, we conducted a search for new variable stars among recent Transiting Exoplanet Survey Satellite observations. We have chosen data from the 79th sector and a part of the 77th sector. As the main result, we discovered 191 variable stars with a sufficient signal-to-noise ratio that were not classified as variables before. We classified 43 of them and determined the variability period for 89 objects. In addition, we found an object with highly unusual changes in magnitude (TIC 149623590), for which we encourage further investigation. The objective of this project is to attract new citizen scientists to astronomy by conducting simple research under the supervision of more experienced mentors.

Key words: stars – variables: general

1. Introduction

Searching for new variable stars has been an area where both professional and amateur astronomers can contribute. Student-led research has actually shown that meaningful scientific results are possible when participants are guided through real data analysis, for example, with mentors or supervisors. For example, Percy (2006, 2008) described how high school and undergraduate students

successfully carried out variable star projects, applying time-series analysis and even publishing discoveries such as the first red giant pulsating in two modes. More recently, Chisabi et al. (2025) reported on a student project regarding pulsar timing following a MeerKAT workshop.

Citizen-science projects also demonstrate what is possible when professionals and volunteers work together, as demonstrated by Kostov et al. (2025) in the case of the Transiting Exoplanet Survey Satellite Ricker et al. (2015) TESS Ten Thousand catalog of eclipsing binaries. Our project is much smaller in scale, but these examples show that with proper guidance and checking, contributions from non-professionals can still be reliable and scientifically useful.

Professional surveys have also used TESS data and other archives to expand the known population of variables. Zhou (2025) identified over 11,000 new δ Scuti and γ Doradus stars through systematic light-curve inspection. This paper also shows the use of visual inspection and period analysis; these methods remain effective approaches even in large-scale research.

Our work continues this tradition within a student-driven framework. The research project was designed to involve students and amateur astronomers in astronomical research by guiding them through a structured study. The main objective of the research is to find new variable stars among observations from the TESS space telescope in sectors 77 and 79. In this way, our project connects the educational potential of student research with the previous methodologies of professional surveys.

TESS[1] is a NASA & MIT space mission launched in 2018 to boost the search for exoplanets across the entire sky. TESS has an unusually large and elongated field of view (24 by 96 degrees), which constitutes a single sector of observations. Each sector is continuously observed during 27.4 days, usually with a single 2-4 day gap in the middle of this period. The observations were performed using the 2-minute short cadence (SC) mode for pre-selected targets, which provides $\approx 16,000$ data points (frames) per target per sector. The entire sky is divided into 31 sectors: 13 for each hemisphere and 5 along the ecliptic. More technical details about TESS are presented in Ricker et al. (2015).

The data from this space observatory is also actively used in other branches of astronomy, most notably in asteroseismology, which was suggested even prior to its launch in Campante et al. (2016). Later research, for example Antoci et al. (2019) and Prša et al. (2022) focusing on the eclipsing binaries, undoubtedly confirmed that suggestion.

We decided to use it for the search for new variable stars, as this process is quite simple and does not require years of studying astronomy. Nevertheless, students must have enough knowledge about the subject to be able to conduct the research. Since they have no prior experience of such research, we prepared a series of educational videos and supplementary text materials. They cover the definitions, physical processes, classification, and some aspects of the research

[1] https://tess.mit.edu/observations/

methods. In total, 10 students managed to finish the educational part and join the research itself.

2. Methods and algorithms

In this section, we describe the details of our research methods and software. This project is the second in our student-led research series, and the methodology follows closely from our previous study Dzygunenko et al. (2026), with some minor updates. While the general algorithm is briefly summarized here, we also include new procedures for identifying potential exoplanet transits, which were not considered in the earlier project.

2.1. General procedure

The procedure for each star consisted of the following steps:

1. Check if the star shows any signs of variability on its light curve and if it is astrophysical variability or a non-astrophysical variability in TESS data. A common solution is to perform aperture photometry from the target pixel files.

2. If a star is variable, check if its variability was detected earlier by someone. First, we checked the database SIMBAD and the AAVSO VSX (The International Variable Star Index) catalog, then all available articles about each star. If neither SIMBAD, VSX, nor NASA ADS contains any mentions of variability for this star, we considered it a newly discovered one.

3. If the star is periodic, we tried to estimate its period using the Lomb-Scargle periodogram, implemented in our Python code.

4. If a star is an eclipsing binary, we classified it "by eye," since those variability types are not numerous and are usually easy to distinguish. The "By eye" classification refers to visually identifying the three main types of eclipsing binaries based on the morphology of the light curves: (i) EA (Algol-type) systems show sharp, well-separated eclipses with flat/almost flat intervals in between; (ii) EB (β Lyrae-type) systems exhibit continuous brightness variation with no flat sections due to tidal distortion; and (iii) EW (W UMa-type) systems have short periods and nearly equal, sinusoidal eclipses due to the stars being in contact.

5. If we suspect an exoplanet orbiting around the star, we apply several vetting methods to rule out false positives. They include analyzing aperture masks, pixel-level light curves, centroid motion, background flux variations, and specialized algorithms like TessCentroidVetting.

6. For pulsating variable stars, we first evaluated whether a star could plausibly belong to this class by estimating its absolute magnitude and spectral type. If the parameters matched those typical of known pulsating variables, we then examined whether the observed period, amplitude, and overall light curve shape were consistent with any specific type. As illustrated in Fig. 1, the location of the new variable star TIC 141985410 on the Hertzsprung-Russell diagram confirms its classification as a DSCT (δ Scuti) variable. The source of this figure [2].

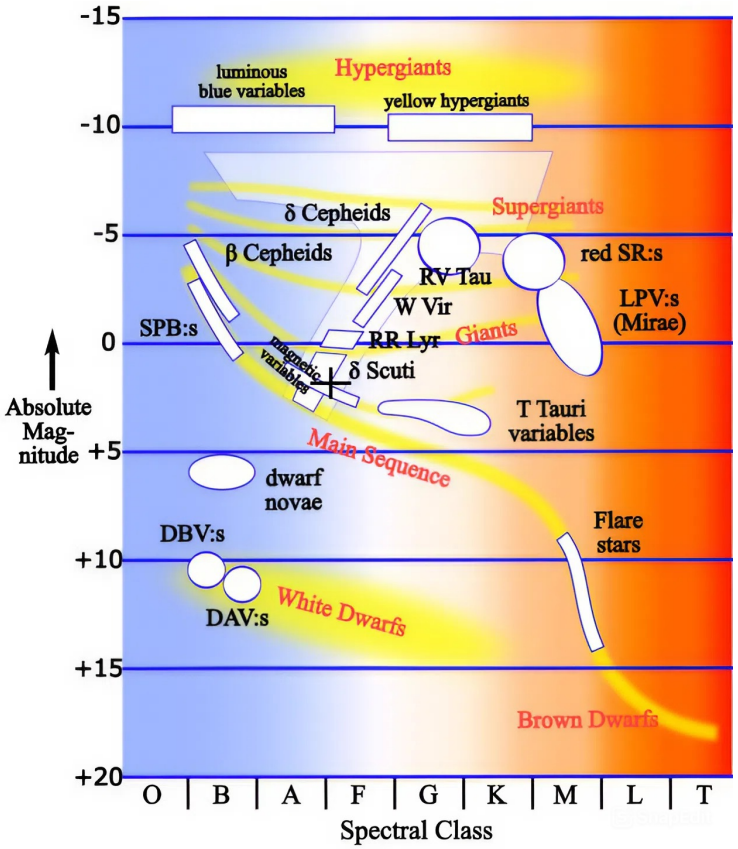

Figure 1. The location of the new variable star TIC 141985410 on the Hertzsprung-Russell diagram, indicated with a + sign.

[2]https://en.wikipedia.org/wiki/Variable_star/media/File:HR-vartype.svg

2.2. Search for exoplanets

Exoplanet transits are a type of variability that was not present in our previous research due to a much smaller number of stars we studied. In this study, we detected 6 light curves, which could be interpreted as exoplanet transits. Despite that, we could not claim a new exoplanet outright because we had to make some checks first. To distinguish real exoplanet transits from false positives, we used the following algorithm, illustrated by TIC 237280203 (Figs. 2 - 7):

1. **Aperture mask analysis.** We examined the authorized aperture masks to ensure the transit signal originates from the target star and not a nearby contaminating source (Fig. 3). Inconsistent transit depths between different masks may indicate a blended eclipsing binary. We used the software developed by Nora Eisner from October 15, 2021 [3], the lightkurve package was used as well [4].

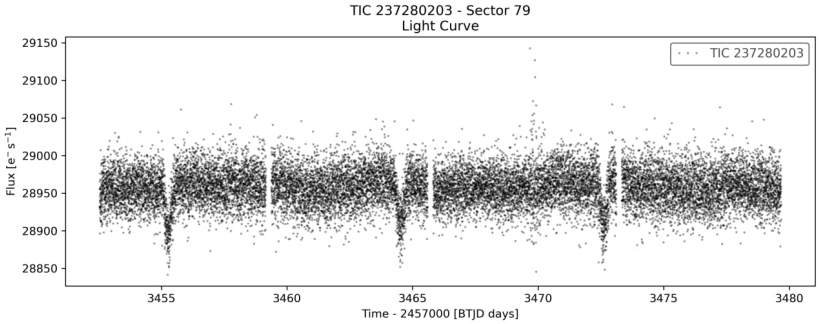

Figure 2. TIC 237280203 as an example for illustration of the algorithm steps.

2. **Pixel-level light curves.** By extracting light curves for each pixel in the target's vicinity, we checked whether the transit signal appears only in the target's pixels (Fig. 4). Dips in neighboring pixels suggest a background eclipsing binary or an instrumental artifact. We used the software developed by Nora Eisner from October 15, 2021 [5].

3. **Centroid motion and satellite motion.** We tracked the position of the brightest pixel during transit events (Fig. 5). Significant centroid shifts imply an off-target origin, such as a nearby eclipsing binary or a moving solar system object. This method was developed by Joseph Twicken and described in Twicken (2019).

[3] https://github.com/noraeisner/PH_Coffee_Chat
[4] https://github.com/lightkurve/lightkurve
[5] https://github.com/noraeisner/PH_Coffee_Chat

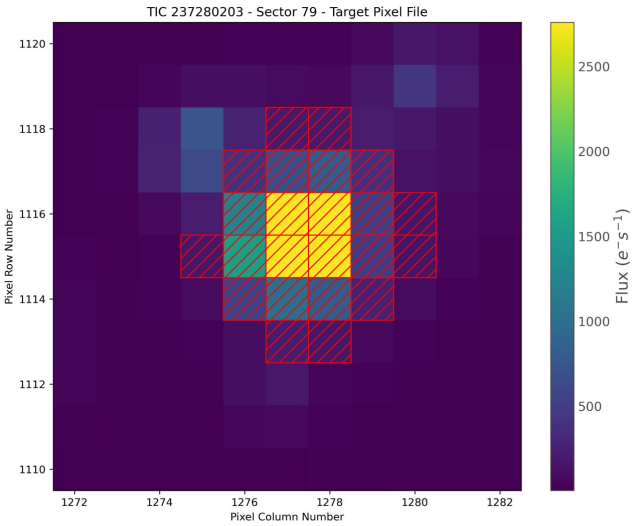

Figure 3. Aperture mask analysis for TIC 237280203. The object is located at the center of the image and corresponds to four yellow pixels.

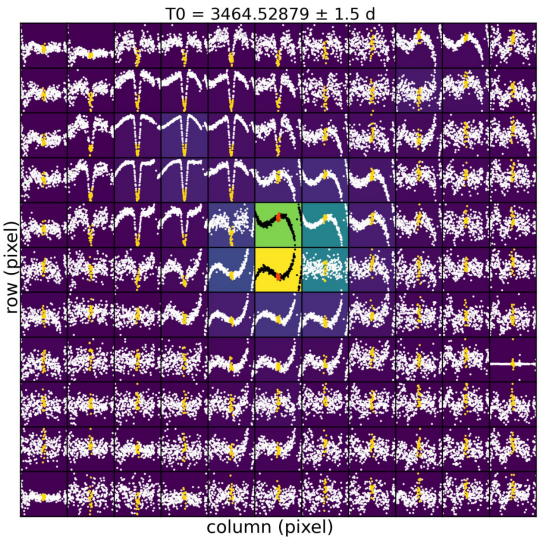

Figure 4. Pixel-level light curves for TIC 237280203. The code computes the flux changes for each individual pixel within close vicinity of the selected object. A group of pixels to the upper left from the center shows clear signs of a background eclipsing binary.

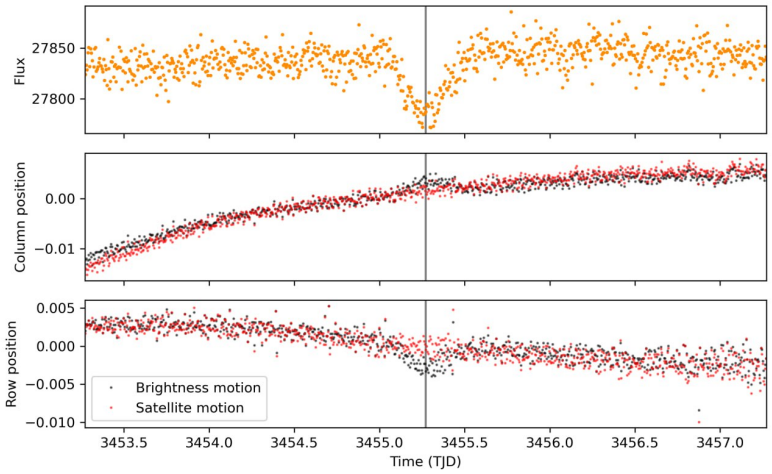

Figure 5. Centroid motion and satellite motion for TIC 237280203. The code analyzes how the position of the brightest pixel shifts along the X-axis (middle panel) and Y-axis (bottom panel) around the timing of a transit (top panel).

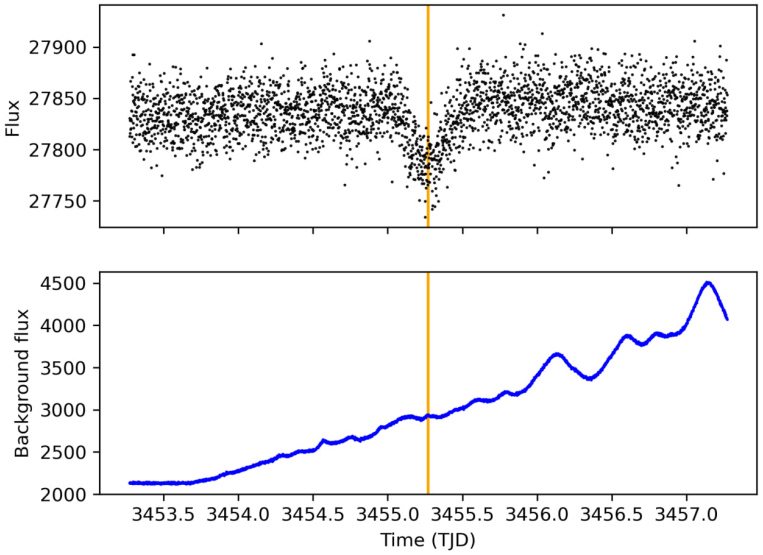

Figure 6. Background flux monitoring for TIC 237280203. In this case the background noise is within the appropriate range.

4. **Background flux monitoring.** Sudden spikes in background flux during transit-like events may indicate contamination from passing solar system objects or scattered light, which could mimic planetary transits (Fig. 6). We used software, developed by Nora Eisner from October 15, 2021 [6].

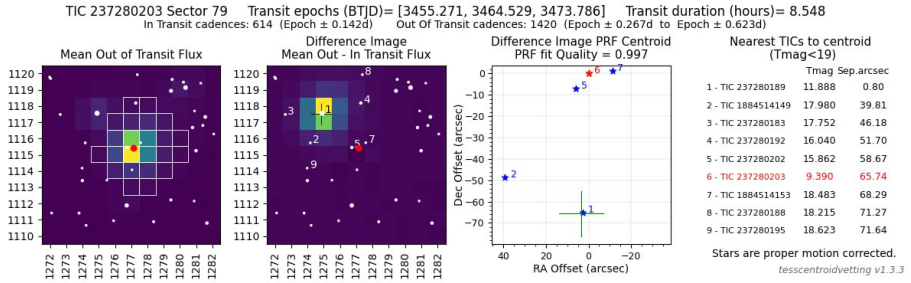

Figure 7. Automated vetting for TIC 237280203.

5. **Automated vetting with TessCentroidVetting.** This algorithm quantitatively evaluates centroid motion during transits, providing statistical confidence in the on-target nature of the signal (see Fig. 7). We used the software "TESS centroid vetting," developed by Rafael Rodrigues and Sam Lee, version 1.3.3. from October 4, 2024 [7].

   However, the periodic dimming can be caused by a stellar spot on the rotating stellar surface. In this case the only tool to determine could be measuring the radial velocities.

Through this multi-stage vetting process, 4 objects out of 6 were confirmed to be false positives (FP). There are background eclipsing binaries (TIC 229458129, TIC 233604585, TIC 237277754, and TIC 237280203). The fifth target (TIC 1400824435) most likely is an eclipsing binary itself because the depth of eclipses on its light curve alternates slightly. The sixth and final signal (TIC 149623590) appears to be of unknown origin and requires further investigation.

2.3. TIC 149623590

TIC 149623590 was by far the most unusual of all variable stars we discovered. It resembles either an exoplanet transit or an Algol-type eclipsing binary with secondary minima not visible due to the gaps in the data (see Fig.8). However, the two minima we could see are significantly asymmetric, which is not typical for both types.

[6] https://github.com/noraeisner/PH_Coffee_Chat
[7] https://github.com/exo-pt/TESS-Centroid_vetting

In total, two minima (T_0=3454.40943 BTJD and T_0=3468.31511 BTJD) were recorded, to which we applied the multi-stage vetting process described in detail in Sec. 2.2, in order to determine whether these signals were caused by astrophysical variability or by systemic trends of the TESS telescope or background flux (e.g., light reflected from the Earth's atmosphere or from objects in our solar system).

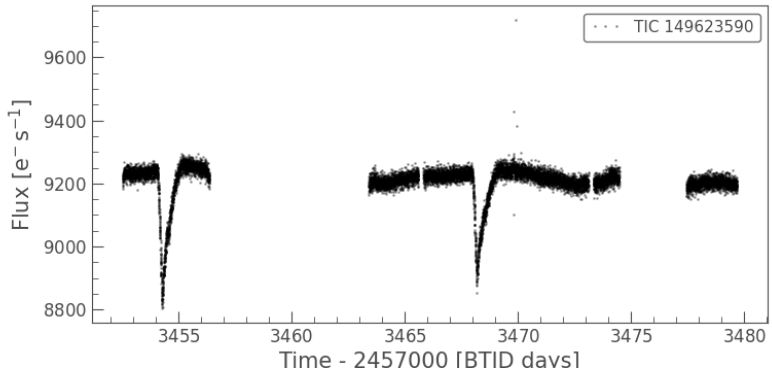

Figure 8. The light curve of the TIC 149623590 in the 79th sector of the TESS observations.

As illustrated in Fig. 9, the photometric aperture fully covers the pixels containing the maximum stellar flux (where our target star is located) and extends to capture several neighboring pixels.

While a background eclipsing binary would typically appear as sinusoidal spikes concentrated within a localized group of pixels, and an object crossing TESS's field of view in the Solar System would show flat-bottomed drops localized to a pixel cluster, Fig. 10 shows that spikes are observed across the entire Target Pixel File (TPF) region, encompassing both the target and the surrounding field. This widespread variability is difficult to reconcile with a purely astrophysical source without additional data.

To investigate the possibility of an instrumental uncertainty, we tracked the centroid during both observed minima (Figs. 11–12). The upper panels of Figs. 11–12 show the asymmetrical shape of the minima in the target flux, while the lower panels display a maximum in brightness motion that corresponds to the time of the star's minima. The same pattern is seen in Figs. 13-14, where we monitored a background flux for both minima, confirming that the signal is originating across the entire TPF area, rather than being isolated to the target aperture.

Finally, the automated vetting procedure shows a gradient in the difference images and formally identified a TIC 149623587 as the source of the signal within

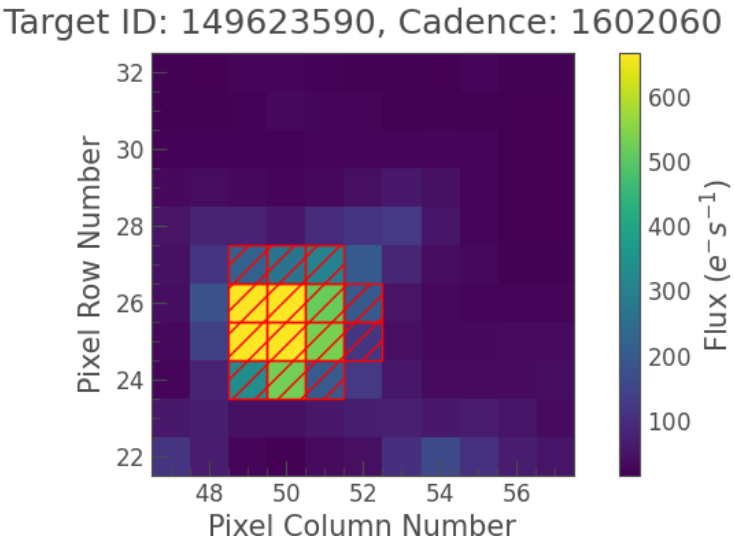

Figure 9. Aperture mask analysis for TIC 149623590. The object is located closer to the left edge of the image and corresponds to four of the brightest yellow pixels.

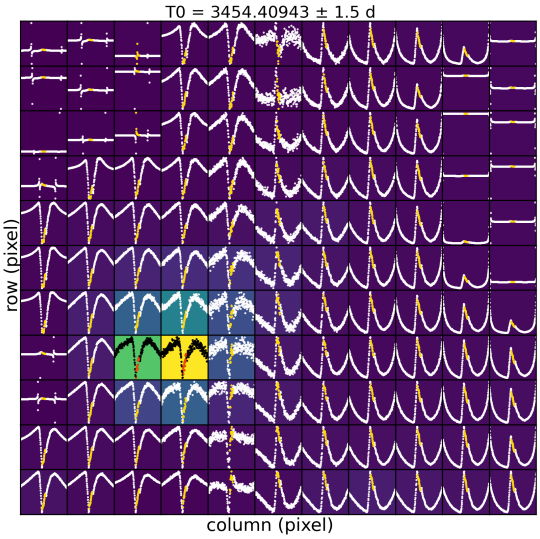

Figure 10. Pixel-level light curves for TIC 149623590. The code computes the flux changes for each individual pixel within close vicinity of the selected object. A whole pixel file shows clear signs of a background source of the signal.

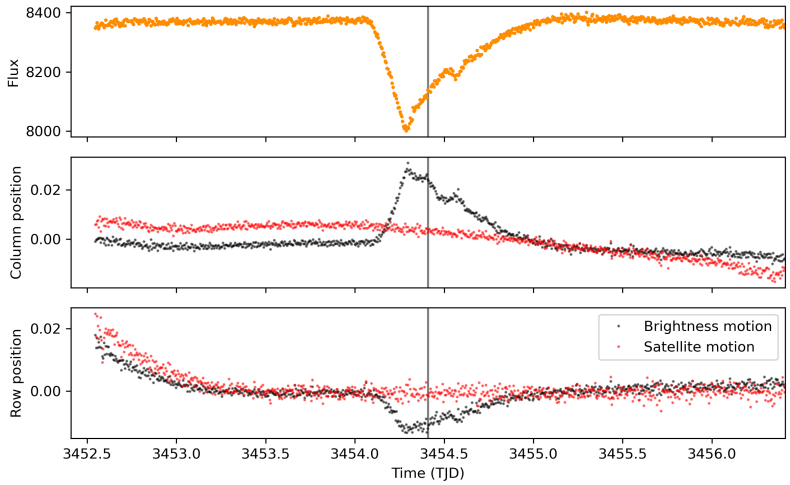

Figure 11. Centroid motion and satellite motion analysis for signal T_0=3454.40943 BTJD on the light curve of TIC 149623590. The code analyzes how the position of the brightest pixel shifts along the X-axis (middle panel) and Y-axis (bottom panel) around the timing of a transit (top panel).

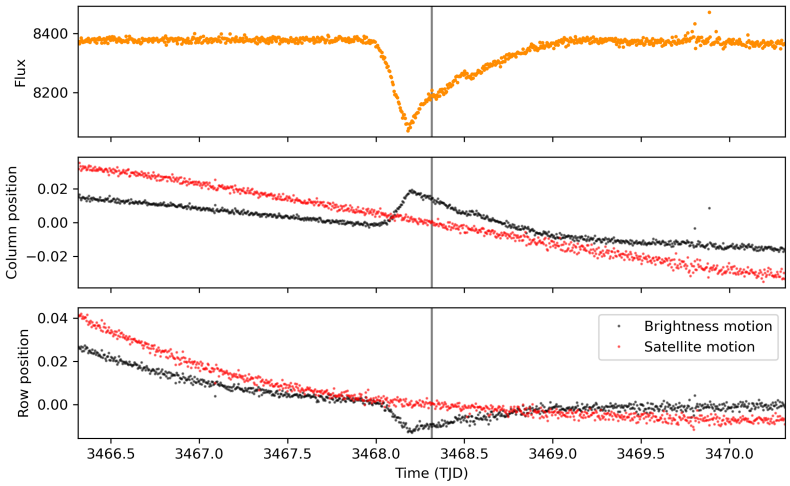

Figure 12. Centroid motion and satellite motion analysis for signal T_0=3468.31511 BTJD on the light curve of TIC 149623590. The code analyzes how the position of the brightest pixel shifts along the X-axis (middle panel) and Y-axis (bottom panel) around the timing of a transit (top panel).

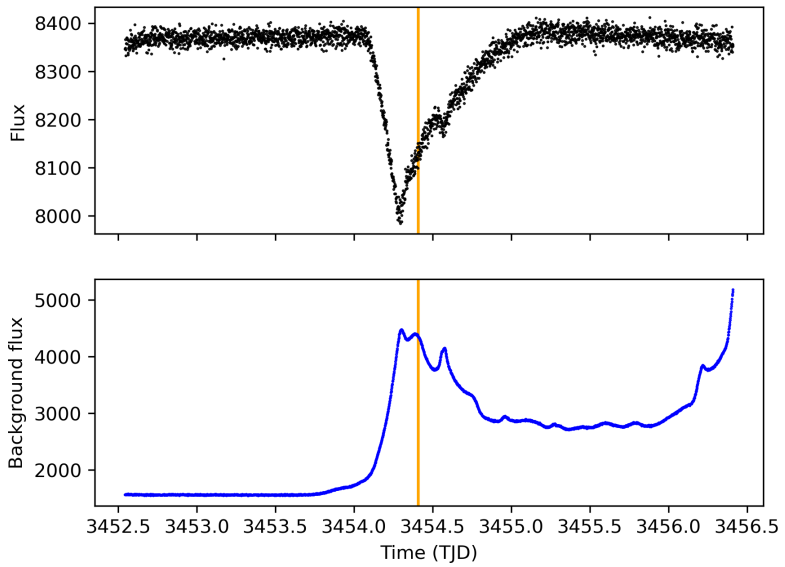

Figure 13. Background flux monitoring for signal T_0=3454.40943 BTJD on the light curve of TIC 149623590.

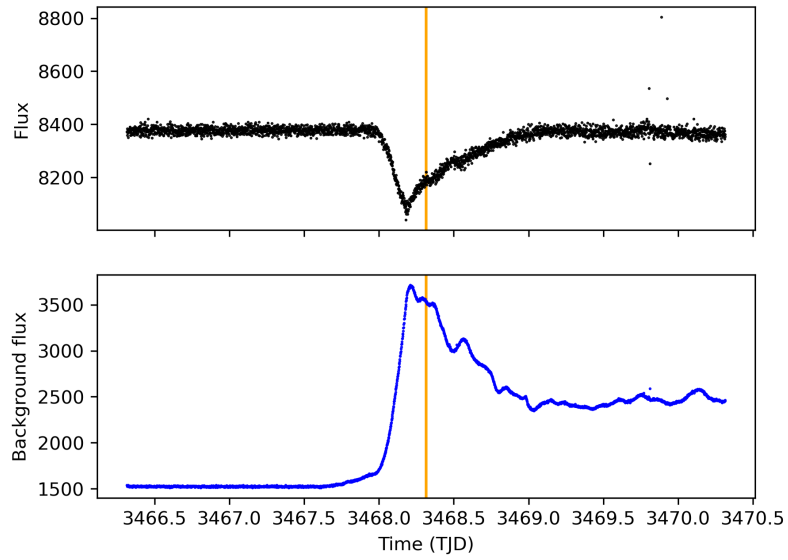

Figure 14. Background flux monitoring for signal T_0=3468.31511 BTJD on the light curve of TIC 149623590.

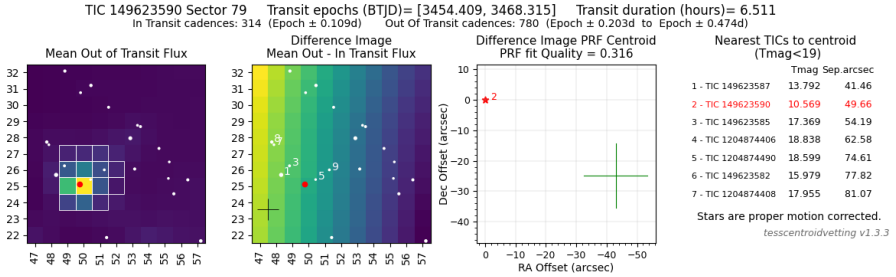

Figure 15. Automated vetting for TIC 149623590.

the TPF. Since there are no other bright variable objects near this star that could cause this complex artifact, we question the reliability of the automated check results, and the source of these minima remains uncertain.

No publicly available spectroscopic observations were found for this object, as well as no additional photometric observations. Thus, we cannot yet determine the type of the object accurately. Moreover, we cannot completely rule out the possibility of an exoplanet or an eclipsing binary system, or that asymmetry is caused by a protoplanetary or accretion disk, since neither of our tests definitively disproved this hypothesis. This object is certainly worth further study, which may lead to noticeable future discoveries.

3. Results

3.1. General table

As the main result, we present a table with 191 newly found variable stars (see Table 1). We managed to calculate periods of 89 of them and estimate classification of 43 objects. If a period is marked as >27, it indicates that the full variability cycle does not fit within a single TESS sector (27.4 days). The asterisk next to the variability type means that the classification for this star is uncertain.

Table 1. List of 191 newly discovered variable stars. The corresponding light curves are displayed in the Appendix (Figs. 16-23). Footnotes elaborate the variability types upon their first appearance in the table.

TIC ID	Variability type	Period	TIC ID	Variability type	Period
7584971	unknown[8]		148049214	DSCT[9]	0.03405
7617177	unknown		148073753	DCEPS[10]	3.87633
7857074	unknown		148119656	unknown	
8347908	unknown	2.12165	148165057	unknown	
9530168	unknown		149690708	unknown	2.65301
10363353	unknown		149693058	unknown	
10473978	unknown	0.3	149736629	unknown	
10491567	unknown		149737192	unknown	
10792081	unknown		149793837	unknown	
11061881	unknown		150486675	unknown	
21028309	unknown		154340851	unknown	
21633694	RRAB[11]	0.33813	154660474	unknown	2.91772
21634379	unknown		154700607	RRD[12]	2.31921
21831633	unknown		154742877	unknown	3.3988
21856856	unknown		154810900	unknown	2.00377
22040779	unknown		154867969	unknown	
22110165	unknown		154874139	unknown	
22113313	unknown		154874588	unknown	5.68367
43276438	CWB[13]	4.07195	229406488	CWB	4.06823
43734727	CWB	5.07478	229458129	FP[14]	1.59619
43794987	unknown	3.60383	229589801	unknown	
43797951	RRD	1.11667	229608810	EA[15]	3.57035
43798687	unknown	1.20601	230137379	RR[16]	1.97426
43870800	unknown		230197161	unknown	6.28467
43908172	DCEPS	5.32061	232529657	unknown	0.8327
44187228	unknown	1.39155	232609078	unknown	
44188129	unknown		232616284	unknown	2.1653
44190078	EA	11.05	233087496	CWA[17]	8.05697

[8]Impossible to definitively identify the variability type.
[9]δ Scuti-type pulsating variable.
[10]δ Cephei-type pulsating variable.
[11]RR Lyrae type pulsating variable, subtype AB.
[12]RR Lyrae-type pulsating variable, subtype D.
[13]BL Herculis-type stars, a subtype of W Virginis variables.
[14]False positive: an exoplanet transit-like signal, but not an exoplanet after further inspection.
[15]β Persei-type eclipsing binary.
[16]RR Lyrae-type pulsating variable, subtype unknown.
[17]W Virginis-type variable star.

Table 1. Continued.

TIC ID	Variability type	Period	TIC ID	Variability type	Period
44267585	EA	>27	233098381	unknown	2.41891
44270304	DSCT*[18]	0.34392	233120677	unknown	1.04069
44386100	unknown	1.45108	233125012	unknown	
44386592	unknown	1.77354	233199626	unknown	10.74
75625642	RR	4.62289	233373166	unknown	
75652037	unknown		233394432	RRC[19]	
75727889	unknown	5.29078	233497034	unknown	
75832705	unknown		233508020	unknown	
75963868	unknown		233526133	unknown	
76138761	unknown	1.88384	233539654	CWB	4.13077
76143193	unknown		233573215	unknown	0.76934
76196131	unknown		233603364	EB[20]	6.62956
82359031	unknown		233604585	FP	3.14164
82408526	unknown		233616650	unknown	1.83426
82599979	unknown		233628452	DSCT	0.36434
82611261	unknown	7.33256	233631689	unknown	
85511656	unknown	1.80732	233633066	DSCT	0.10513
85743873	unknown		233650118	unknown	4.04771
88840705	unknown		233730340	unknown	
88877401	unknown		233790846	unknown	
88995742	unknown		235596189	unknown	
99543677	unknown		235711657	unknown	7.7032
101675157	unknown	5.21821	235712705	unknown	
102988612	unknown		235947146	unknown	
103096562	unknown	1.22781	235980310	unknown	
103179478	unknown		236001714	CWB	6.40481
103194937	unknown		236010034	unknown	5.2
103508168	unknown	1.42066	236013234	unknown	
103565392	unknown		236393296	unknown	
115183789	unknown	2.04017	236750863	unknown	
115288430	unknown		236752232	unknown	
115611128	unknown	0.88966	236770582	RRC	4.86927
116048705	unknown		237119483	unknown	
116097246	unknown		237132577	unknown	
116126490	unknown		237133525	unknown	
116164903	unknown		237277754	FP	0.7048

[18] An asterisk means classification is uncertain.
[19] RR Lyrae-type pulsating variable, subtype C.
[20] β Lyrae-type eclipsing binary.

Table 1. Continued.

TIC ID	Variability type	Period	TIC ID	Variability type	Period
116241468	RR	0.87532	237280203	FP	9.23
122789619	unknown	1.71742	237285047	unknown	
122890144	unknown		243335760	unknown	
123091906	unknown		416053615	SRs[21]	8.02145
137083163	unknown		416099134	unknown	7.33382
137086255	unknown	0.52792	416102581	DSCT	0.06352
137479673	unknown		416120082	unknown	
137995653	RVA*[22]	2.55983	416124077	unknown	
138026606	DCEPS	4.23973	416125133	RR	2.61754
138046660	unknown	2.94937	417617028	unknown	
138107363	RRC		417620193	unknown	
138108399	unknown	1.67503	417703706	RRD	0.5424
138121408	unknown		417746470	unknown	
138471905	DCEP	9.69081	418111831	unknown	2.51609
140737856	unknown	9.3567	418372012	unknown	
141533678	unknown		420456245	unknown	
141917304	unknown		420536861	unknown	
141950998	unknown		420729120	unknown	
141983134	unknown	1.09414	420801643	unknown	
141985410	DSCT	0.05264	423029433	unknown	
142010247	unknown		424731804	unknown	2.85634
142043413	unknown	0.75373	427029032	unknown	
142677896	RRC	0.3293	428772395	RR	1.11988
143036407	unknown	3.0318	428888603	unknown	
143062447	RR	2.26121	435741597	unknown	
143100422	unknown	1.40594	435741713	CWB	4.07405
143162957	unknown		441720037	unknown	2.95963
143185397	unknown		441789740	unknown	
143185490	unknown	2.60911	441808062	unknown	4.0682
147716003	unknown		1400824435	EB	2.16605
147751796	unknown		149623590	unknown	
147752402	CWB	3.08347			

[21] Semi-regular variable star.

[22] RV Tauri-type variable, subtype A.

3.2. Period uncertainty estimation

To roughly estimate uncertainty s of our calculations for the period, we conducted a test. This test involved creating artificial datasets, similar to TESS observations: sine waves with a random amplitude, period, and noise. Each dataset is exactly 1 sector (27.4 days) long with a 2-5 day gap in the middle and a 2-minute interval between data points. The period of the sine wave was in the range from 0.1 to 50 days. In total, we generated 500 TESS-like sectors. We ran each of them through the Lomb-Scargle algorithm to compute the period and calculate the percentage difference between real and calculated periods.

As a result, we have realized that accuracy decreases rapidly for longer periods, since fewer and fewer sine waves could fit into a single sector. For example, stars with periods less than 2 days have typical uncertainty of 0.005-0.1%. Stars with periods of 2-10 days have uncertainty s of about 0.1-0.6%. With a period approaching the duration of a sector (27.4 days), uncertainty increases to 0.8-1.2%, and for periods of 40-50 days, uncertainty could reach as much as 3%, which is an inappropriately large uncertainty for variable stars. We note that the calculated uncertainty do not decrease with an increasing number of points on the Lomb-Scargle diagram after a certain point. We have tested 1000, 3000 and 10 000 points per diagram, giving us almost the same results.

4. Discussion and Conclusions

The main purpose of this research was educational. We trained students to work with real TESS data. They watched specially prepared videos about basic aspects of variable stars and their research, read our manuals, and practiced with already classified light curves before working with new observations. More experienced researchers supervised their progress and checked the results. Students also could use obtained knowledge in their future research. However, the dropout rate during the initial stages was much higher than expected, which made us review our approach to teaching.

From a scientific perspective, we also faced several challenges. The first was to quickly search across hundreds of stars viewed by students. We had to confirm that all objects they marked as "new variable stars" are indeed new and variable, which appeared to be easier said than done. We checked the variability of the stars manually by analyzing their light curves. We excluded light curves with very high noise and only accepted those with a clear and reliable signal. For the other part, we made a code in Python, which searches for keywords related to variable stars in articles and in SIMBAD and AAVSO VSX for each star. It significantly reduced the amount of time and effort required for the process. In total, over 300 claimed stars were rejected because of either having a too low signal-to-noise ratio or being discovered previously. We also found out that if an article indexed in NASA ADS is not yet connected to SIMBAD, it may lead to a temporary mismatch in the classification and repetitive discoveries.

The second tough challenge was classification. While eclipsing binaries were easy to classify, pulsating variables proved to be anything but. Since we were limited to using only light curves and radial velocities were not available for the vast majority of the stars, we were not able to classify more than half of the stars at all. Many types of pulsating stars have similar light curves; moreover, their shapes also match some types of rotating variable stars. To avoid providing a false classification, we tried to check if a star at least could be a pulsating variable. We used tools such as the Hertzsprung–Russell diagram along with established formulas—Ballesteros' for temperature and Pogson's for magnitude—to improve our confidence in classifying variable stars. Although it helped, the classification of pulsating stars remained especially challenging, and some uncertainty remains. To avoid misleading further research, any star whose light curve and corresponding parameters did not clearly match established types was marked as unknown. The total number of stars marked as unknown is 148.

Based on our experience, attracting new students to astronomy using simple research is possible and quite efficient, considering the moderate amount of effort it required. The project successfully joined scientific research with education by giving students hands-on experience with real TESS data—from detecting variability to validating classifications. However, both the educational part and the actual research should be improved for the future projects. Using semi-automated tools could help measure important features of the light curves while still allowing for manual checks. Although our method was partially manual, it yielded significant new data for the astronomical community for further analysis and use. Overall, while our current semi-automated method was successful for analyzing periodic variable stars, improving our approach will be important to increase both accuracy and the variety of objects we could study.

Acknowledgements. This paper includes data collected with the TESS mission, obtained from the MAST data archive at the Space Telescope Science Institute (STScl). Funding for the TESS mission is provided by the NASA Explorer Program. STScl is operated by the Association of Universities for Research in Astronomy, Inc., under NASA contract NAS 5-26555. This research was conducted as the first part of the TESS-UA-2024 research project for young scientists, organized by the Clear Skies Foundation.

References

Antoci, V., Cunha, M. S., Bowman, D. M., et al., The first view of δ Scuti and γ Doradus stars with the TESS mission. 2019, *Monthly Notices of the RAS*, **490**, 4040, DOI:10.1093/mnras/stz2787

Campante, T. L., Schofield, M., Kuszlewicz, J. S., et al., The Asteroseismic Potential of TESS: Exoplanet-host Stars. 2016, *Astrophysical Journal*, **830**, 138, DOI:10.3847/0004-637X/830/2/138

Chisabi, M., Andrianomena, S., Enwelum, U., et al., Timing and noise analysis of five millisecond pulsars observed with MeerKAT. 2025, *Monthly Notices of the Royal Astronomical Society*, **537**, 2462, DOI:10.1093/mnras/staf100

Dzygunenko, A., Yatsiuk, M., Popenko, M., et al., New variable stars from TESS sector 86. 2026, *Journal of Physical Studies*, **30**, 1901, DOI:10.30970/jps.30.1901

Kostov, V. B., Powell, B. P., Fornear, A. U., et al., The TESS Ten Thousand Catalog: 10,001 Uniformly Vetted and Validated Eclipsing Binary Stars Detected in Full-frame Image Data by Machine Learning and Analyzed by Citizen Scientists. 2025, *The Astrophysical Journal Supplement Series*, **279**, 50, DOI:10.3847/1538-4365/ade2d8

Percy, J. R., Variable Star Research Projects for Outstanding Senior High School Students. 2006, *Journal of the American Association of Variable Star Observers*, **35**, 284

Percy, J. R., Variable Star Research Experiences for High School Students, Undergraduates, and Amateur Astronomers. 2008, in Astronomical Society of the Pacific Conference Series, Vol. **400**, *Preparing for the 2009 International Year of Astronomy: A Hands-On Symposium*, ed. M. G. Gibbs, J. Barnes, J. G. Manning, & B. Partridge, 363

Prša, A., Kochoska, A., Conroy, K. E., et al., TESS Eclipsing Binary Stars. I. Short-cadence Observations of 4584 Eclipsing Binaries in Sectors 1-26. 2022, *The Astrophysical Journal Supplement Series*, **258**, 22, DOI:10.3847/1538-4365/ac324a

Ricker, G. R., Winn, J. N., Vanderspek, R., et al., Transiting Exoplanet Survey Satellite (TESS). 2015, *Journal of Astronomical Telescopes, Instruments, and Systems*, **1**, 014003, DOI:10.1117/1.JATIS.1.1.014003

Twicken, J. 2019, Data Validation: Difference Imaging and Centroid Analysis, https://ntrs.nasa.gov/api/citations/20190029148/downloads/20190029148.pdf, [Online; accessed 10-December-2025]

Zhou, A.-Y., Variability Census of Legacy Catalogs. V. 11,820+ New δ Scuti and γ Doradus Stars. 2025, *Research Notes of the AAS*, **9**, 145, DOI:10.3847/2515-5172/ade301

A. Light curves of newly identified variable stars

All TESS light curves for the 191 newly identified variable stars are shown below. Each figure presents a grid of 24 light curves (8×3), labeled with TIC IDs above each panel. The numbers in the captions indicate the object index range corresponding to Table 1.

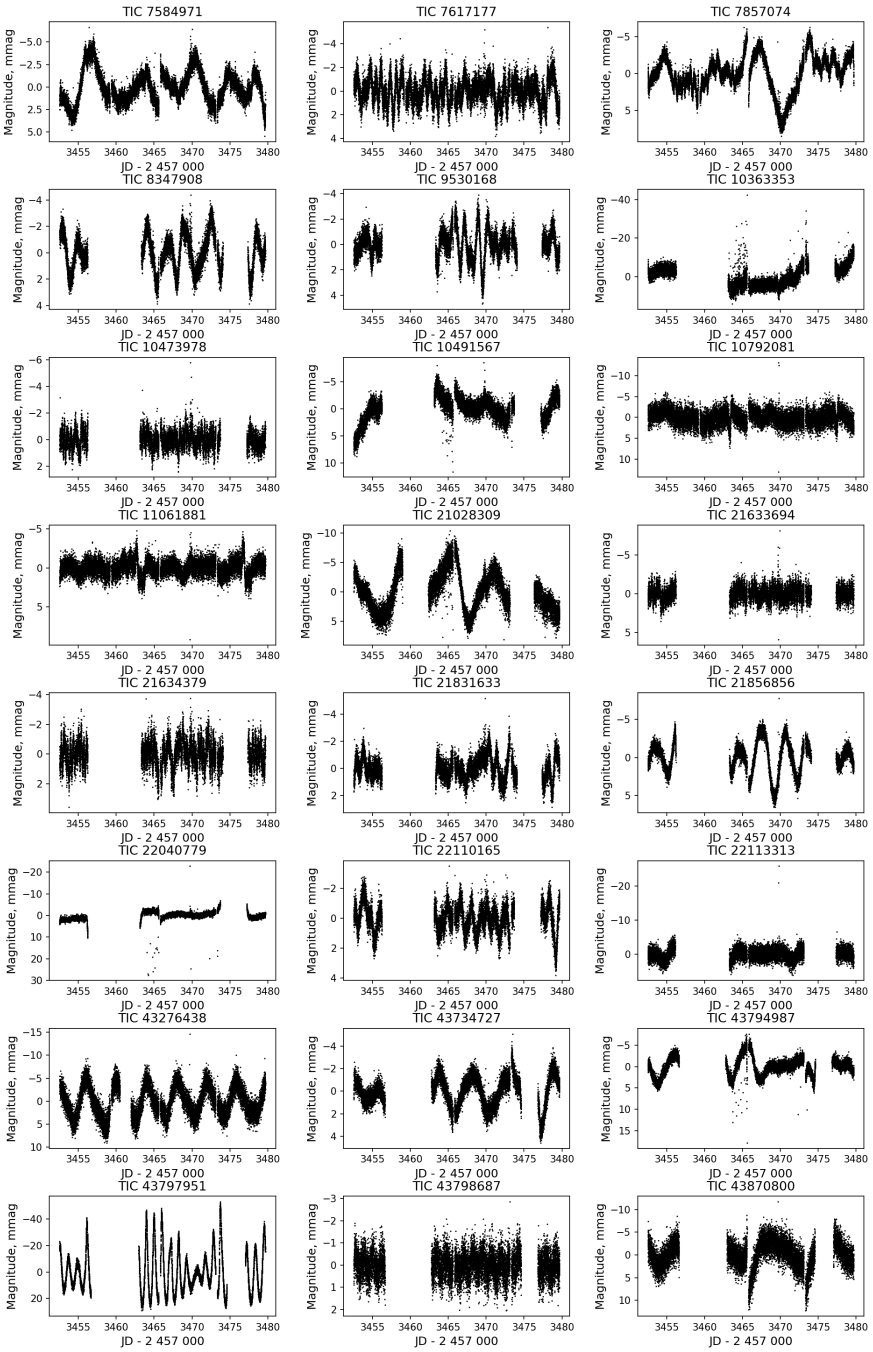

Figure 16. Grid of light curves for objects 1–24.

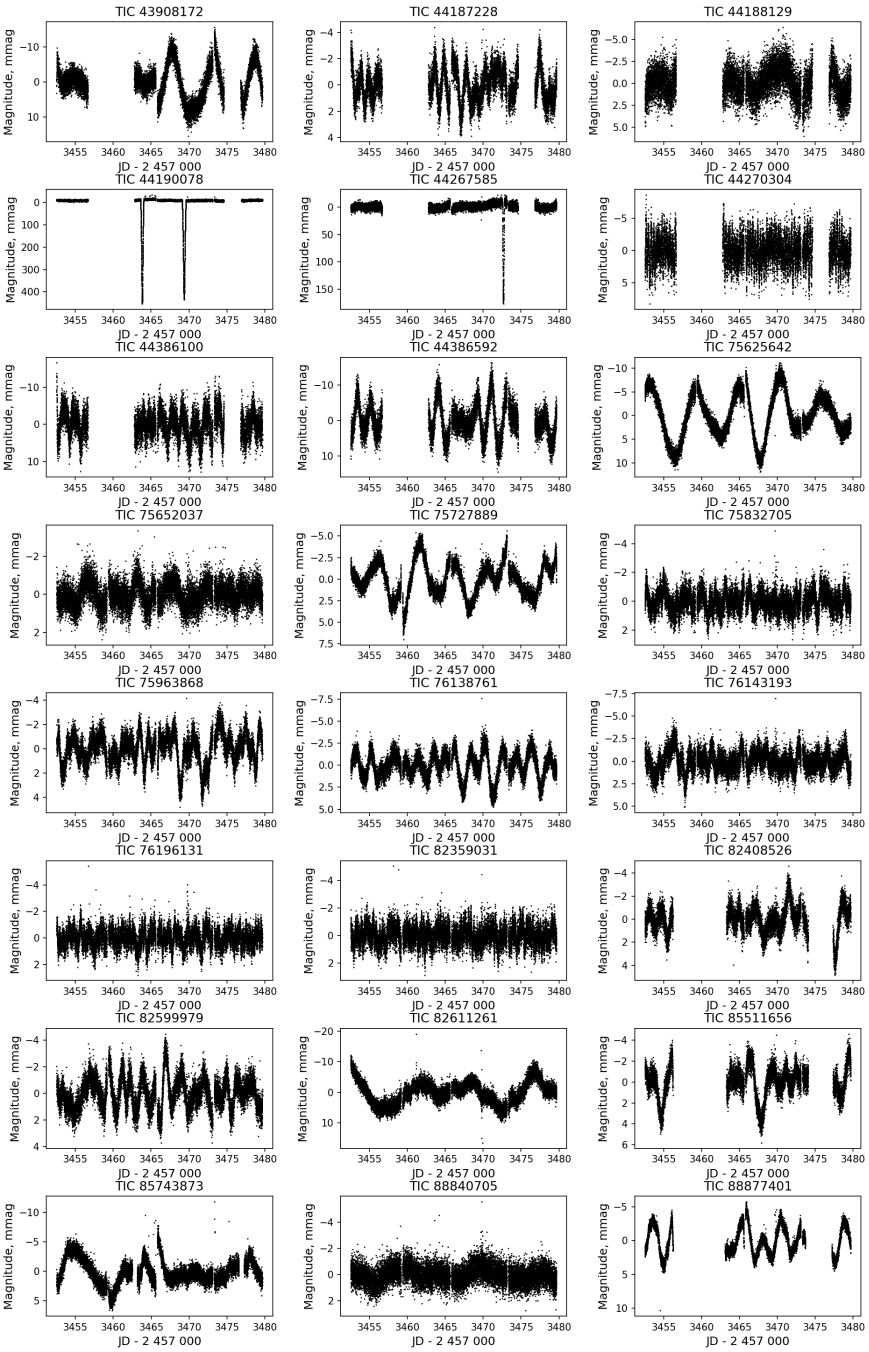

Figure 17. Grid of light curves for objects 25–48. Continued.

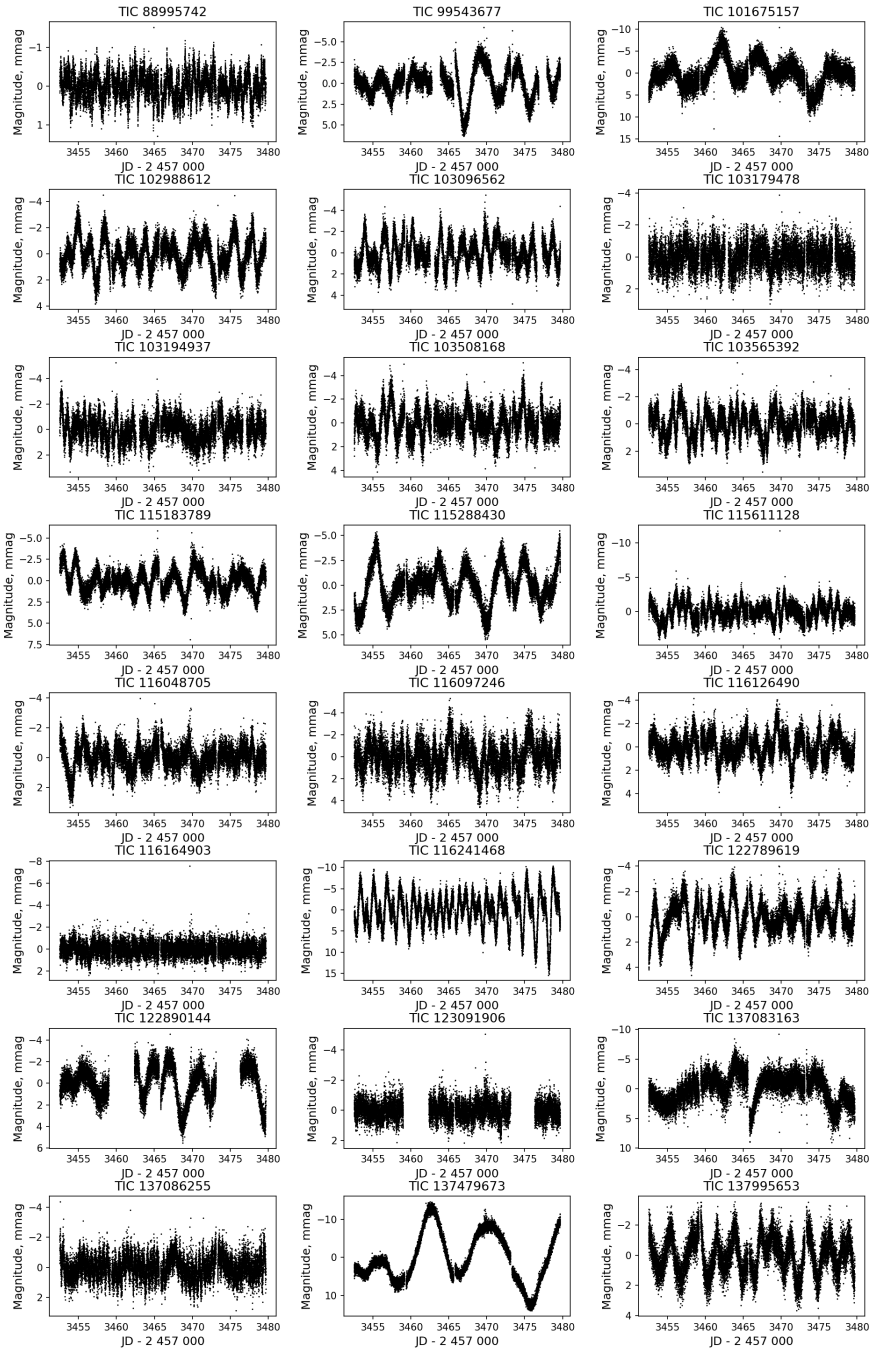

Figure 18. Grid of light curves for objects 49–72. Continued.

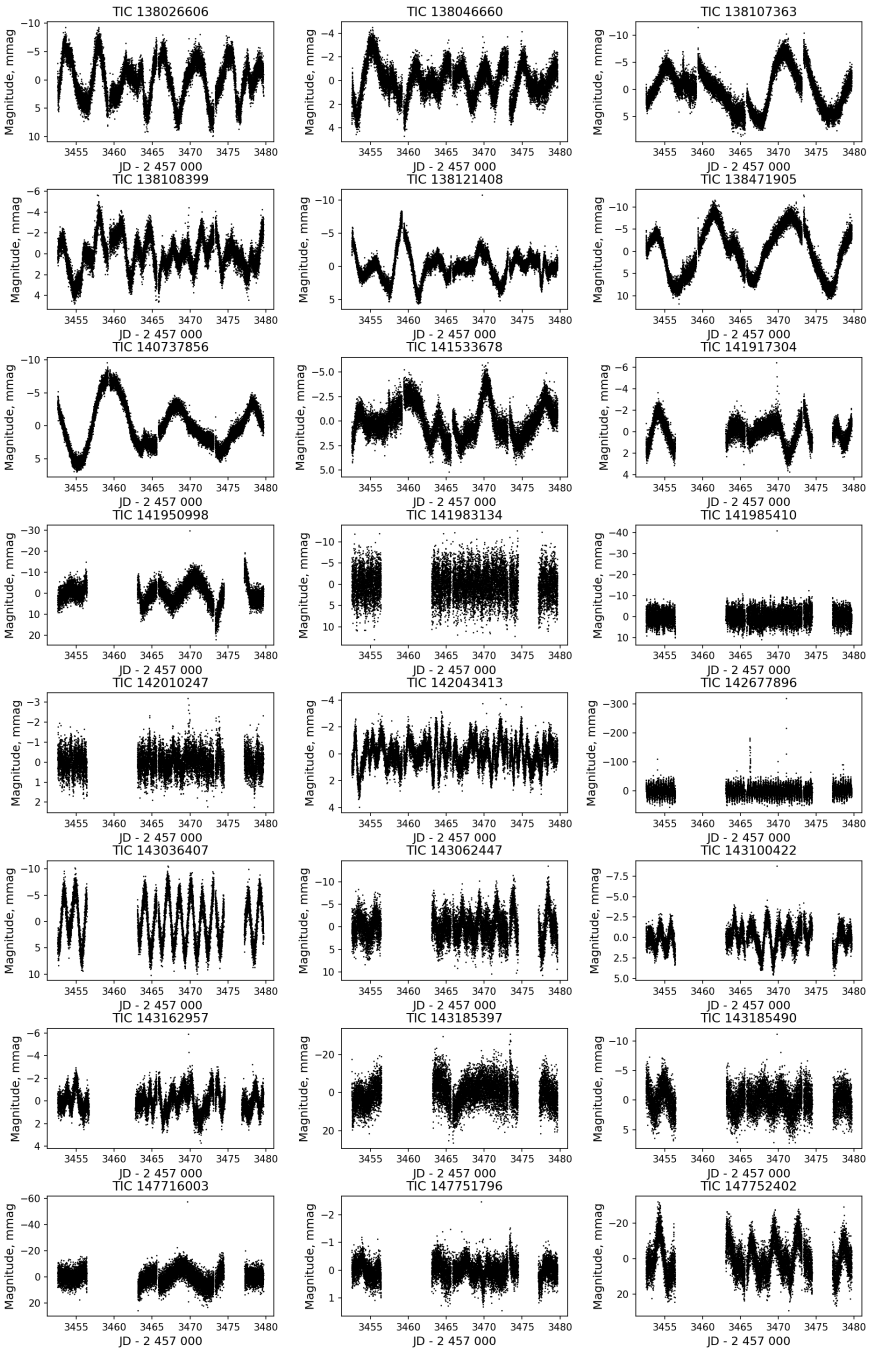

Figure 19. Grid of light curves for objects 73–96. Continued.

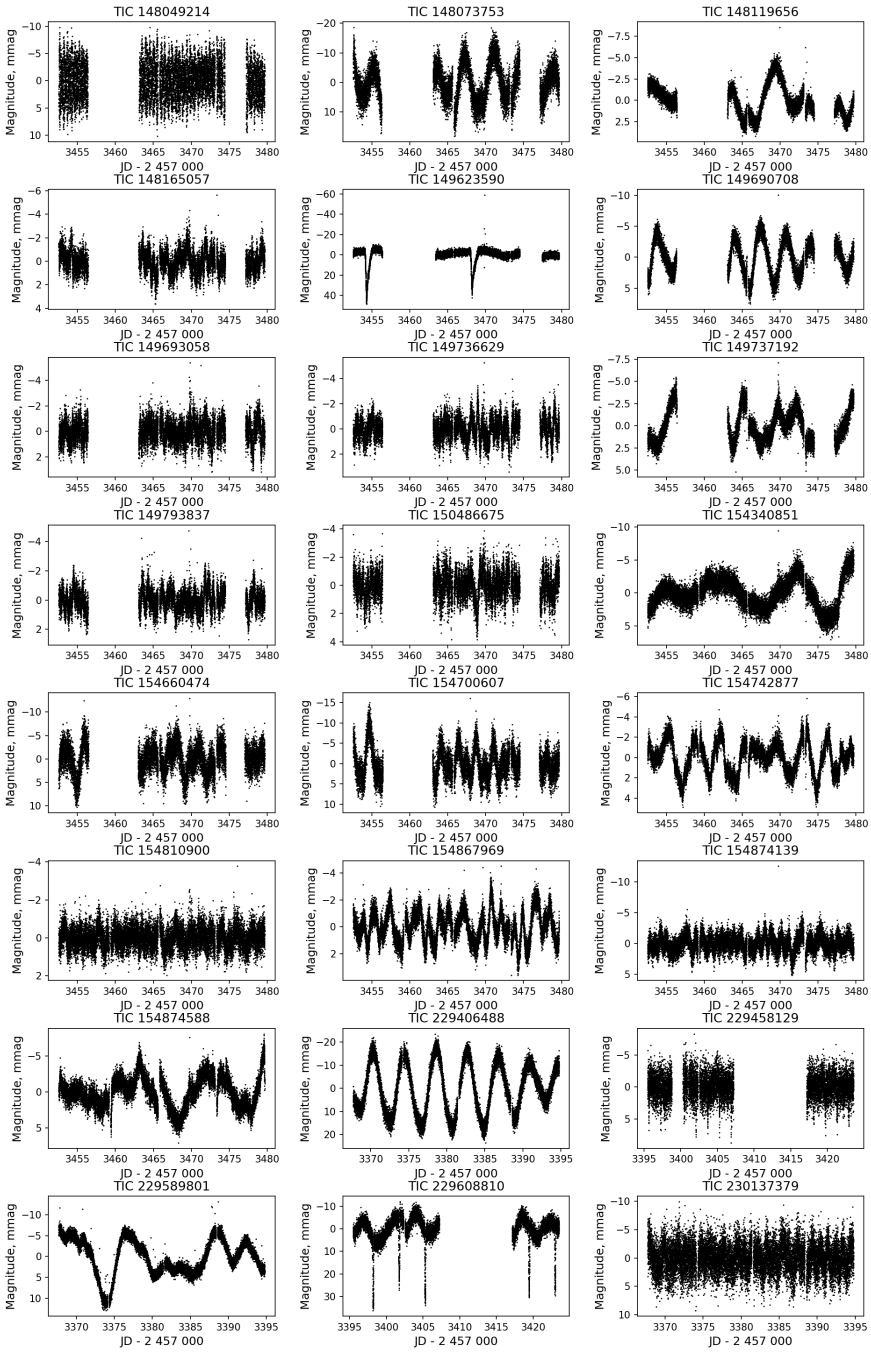

Figure 20. Grid of light curves for objects 97–120. Continued.

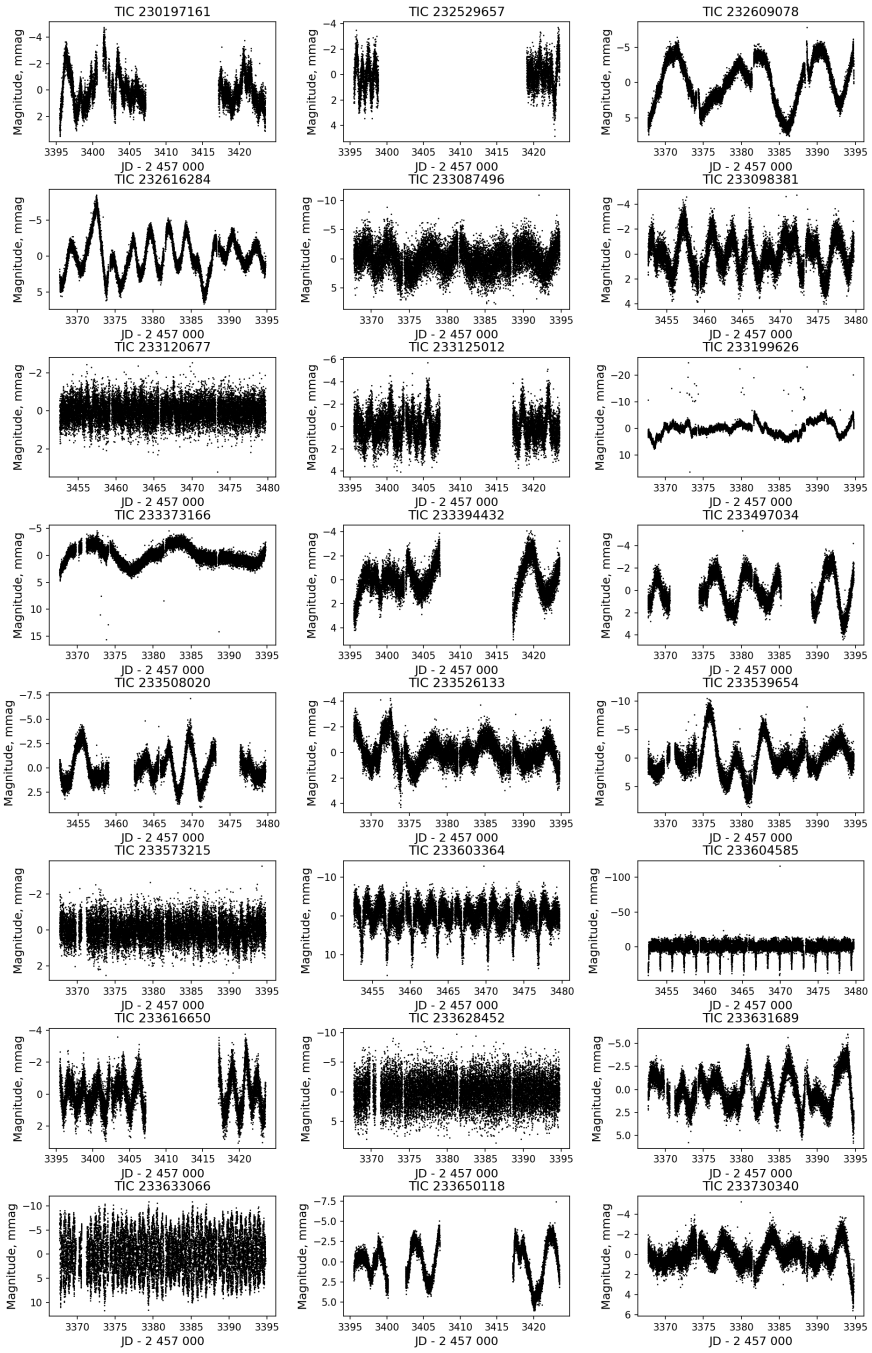

Figure 21. Grid of light curves for objects 121–144. Continued.

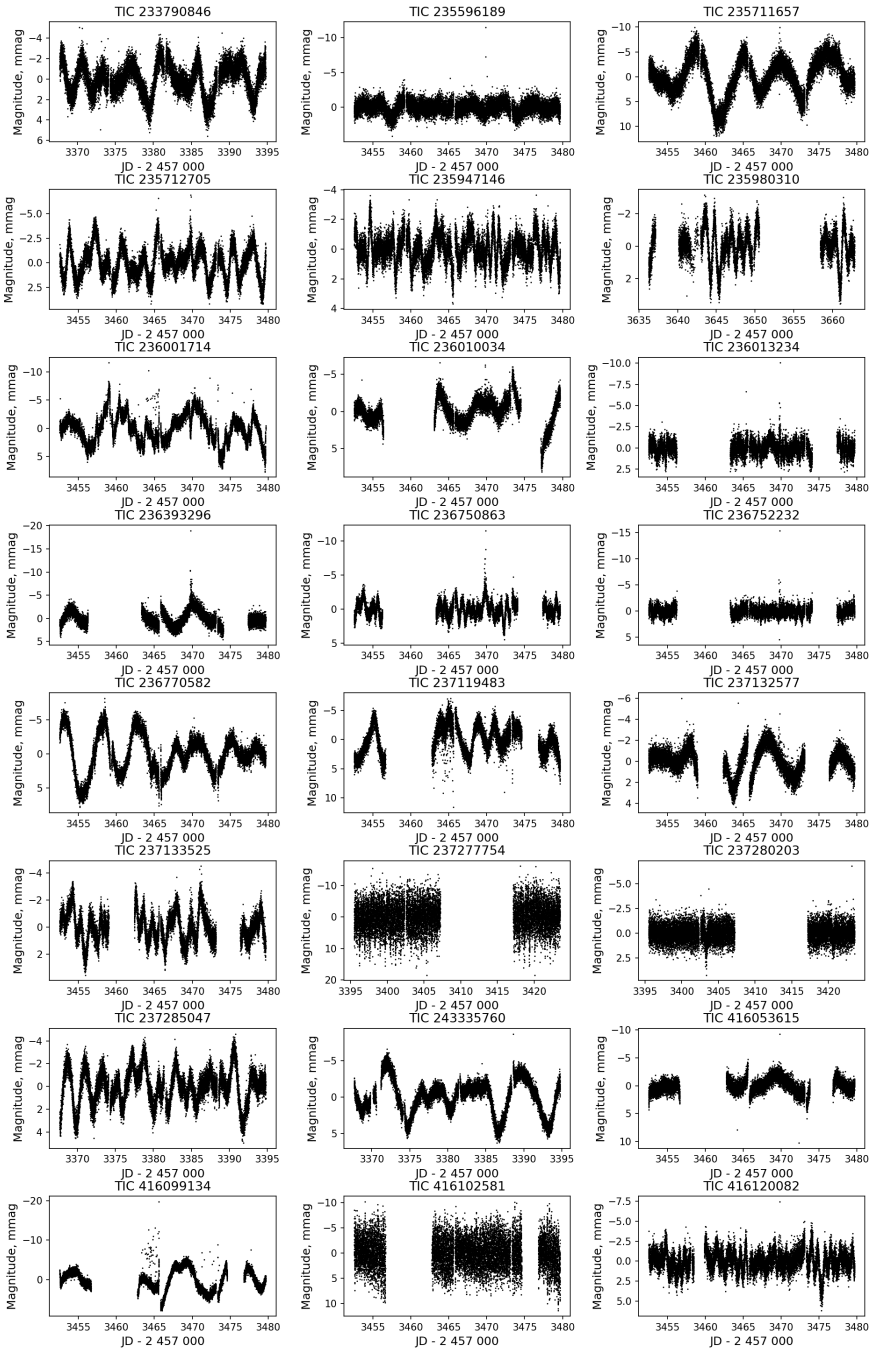

Figure 22. Grid of light curves for objects 145–168. Continued.

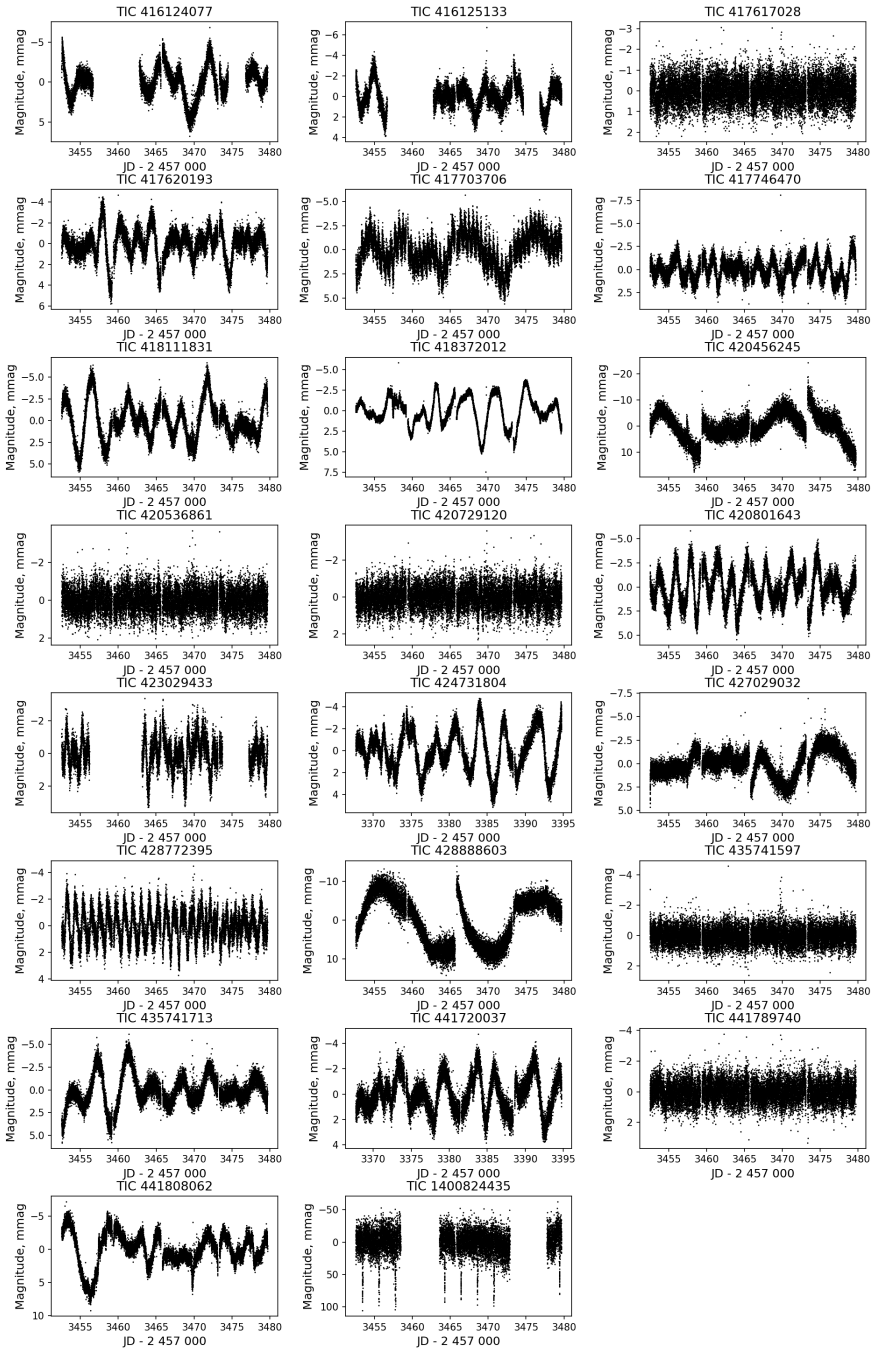

Figure 23. Grid of light curves for objects 169–191. Continued.